

AD-A050 145

CALIFORNIA INST OF TECH PASADENA DIV OF CHEMISTRY A--ETC F/G 20/12  
HIGH-RESOLUTION, SOLID STATE NMR. (U)

JAN 78 R W VAUGHAN  
TR-7

N00014-75-C-0960  
NL

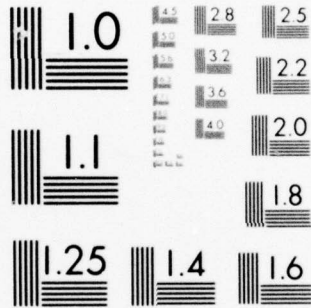
UNCLASSIFIED

| OF |

AD  
A050145



END  
DATE  
FILMED  
3-78  
DDC



MICROCOPY RESOLUTION TEST CHART  
NATIONAL BUREAU OF STANDARDS-1963-A

Unclassified

SECURITY CLASSIFICATION OF THIS PAGE (When Data Entered)

12

AD A 050 145

AD No. DDG FILE COPY

REPORT DOCUMENTATION PAGE		READ INSTRUCTIONS REPORT COMPLETING FORM
1. REPORT NUMBER <b>Technical Report #7</b>	2. GOVT ACCESSION NO.	3. REPORT TYPE & EXTENT
4. TITLE (and Subtitle) <b>HIGH-RESOLUTION, SOLID STATE NMR</b>	5. TYPE OF REPORT & PERIOD COVERED <b>interim, Technical Report #7</b>	6. PERFORMING ORG. REPORT NUMBER
7. AUTHOR(s) <b>Robert W. Vaughan</b>	8. CONTRACT OR GRANT NUMBER(s) <b>N00014-75-C-0960</b>	9. PROGRAM ELEMENT, PROJECT, TASK AREA & WORK UNIT NUMBERS <b>NR-056-605</b>
10. PERFORMING ORGANIZATION NAME AND ADDRESS <b>Division of Chemistry &amp; Chemical Engineering California Institute of Technology Pasadena, California 91125</b>	11. CONTROLLING OFFICE NAME AND ADDRESS <b>ONR Branch Office ATTN: Dr. R. J. Marcus 1030 East Green Street Pasadena, California 91106</b>	12. REPORT DATE <b>1/78</b> <b>11 June 78</b>
13. MONITORING AGENCY NAME & ADDRESS (if different from Controlling Office)	14. NUMBER OF PAGES <b>62</b> <b>12/154 p.</b>	15. SECURITY CLASS. (of this report) <b>Unclassified</b>
16. DISTRIBUTION STATEMENT (of this Report) <b>Approved for public release; distribution unlimited</b>		17. DISTRIBUTION STATEMENT (of the abstract entered in Block 20, if different from Report) <b>DDC RECEIVED FEB 17 1978 RESERVED F</b>
18. SUPPLEMENTARY NOTES <b>Submitted for publication, Annual Review of Physical Chemistry</b>		
19. KEY WORDS (Continue on reverse side if necessary and identify by block number) <b>NMR interferometry, double resonance, nuclear magnetic resonance, spin dynamics, spinor character, sample spinning, polarization transfer, dipolar couplings, polycrystalline solids, benzene</b>		
ABSTRACT (Continue on reverse side if necessary and identify by block number) <b>A review of the experimental capabilities presently available for the modification of spin Hamiltonians normally encountered in solids has been presented to illustrate the control the still-developing high-resolution, solid state NMR techniques furnish. Examples have been discussed to furnish insight into how such schemes can be used to control the time development of a nuclear spin system to allow a detailed characterization of both the electronic and molecular-frame structure near a nuclear site. While the examples specifically discussed have been chosen from areas of current activity, they are only</b>		

DD FORM 1473 1 JAN 73

EDITION OF 1 NOV 65 IS OBSOLETE S/N 0102 LF 014 6601

Unclassified

SECURITY CLASSIFICATION OF THIS PAGE (When Data Entered)

071575

slh

20. cont.

examples of present efforts, and future developments in this field will undoubtedly furnish many more such examples since the concepts upon which these techniques are based are quite general, and there exists great flexibility for the development of specific experimental schemes for a given problem.

HIGH-RESOLUTION, SOLID STATE NMR

by

Robert W. Vaughan  
Division of Chemistry and Chemical Engineering  
California Institute of Technology  
Pasadena, California 91125  
(213) 795-6811, ext. 1183

ACCESSION for	
NTIS	W. I. Section <input checked="" type="checkbox"/>
DDC	B. I. Section <input type="checkbox"/>
UNANNOUNCED	<input type="checkbox"/>
J. S. I. I. I. I.	
BY	
DISTRICT/REGIONAL AGENCY NOTES	
DATE	
A	

## Table of Contents

	<u>Page</u>
Introduction	1
Background	4
The Dipolar Hamiltonians	9
The Chemical Shift Hamiltonian	12
The Quadrupolar Hamiltonian	16
More Complex Characterization Schemes	20
Sample Spinning; Chemical Shifts	20
Correlation of Dipolar and Chemical Shift Hamiltonians	25
Heteronuclear Dipolar vs. Dilute-spin Chemical Shift Hamiltonian	28
Homonuclear Dipolar vs. Abundant-spin Chemical Shift Hamiltonian	35
Final Comments	39
Acknowledgment	40
Literature Cited	41
Figure Captions	46

## INTRODUCTION

Nuclear magnetic resonance (NMR) has long been a useful technique for the characterization of molecular properties in the liquid state, and within recent years there has been a rapid advance in the development of "high-resolution" NMR techniques for characterization of molecular properties of solids (1-7). These still-developing techniques offer at present a means for characterization of both physical and chemical properties within solids in many ways superior to what has been available for liquids through conventional high-resolution NMR. The same interactions are responsible for both the solid state and liquid spectra, with the major difference being that rapid molecular motion averages the various interactions in the liquid case, while one must deal with the more complex, unaveraged Hamiltonians in the case of solids (7,8). The unaveraged (or possibly anisotropically averaged) Hamiltonians have a much higher inherent information content than those fully motionally averaged. However, the additional complexity involved in attempting to unravel and sort the various unaveraged interactions present in solids has been a major impediment to the development of solid state NMR techniques, particularly those directed toward analysis of polycrystalline

solids (9). A number of advances during the past ten years have gradually increased the control one can exercise experimentally to sort and characterize the various Hamiltonians, and at present, these techniques greatly expand the utility of nuclear magnetic resonance NMR as an experimental technique for the study of physical and chemical phenomena in solids.

The present review will attempt to put a portion of these developments into perspective with particular emphasis on those capabilities which are allowing detailed characterization of polycrystalline materials. A focus of the discussion below will be to illustrate several different examples of general schemes which, rather than simply unraveling the complex Hamiltonians present, allow one to correlate, or modulate, one interaction with a second and thus recover much of the orientational information normally lost in dealing with polycrystalline samples.

The reader is referred to a monograph by Mehring (1) for a comprehensive development of the theoretical basis for the high-resolution experimental techniques. Haeberlen (2) has reviewed the homonuclear multiple-pulse techniques, while in somewhat older reviews Andrew (5) has discussed sample-spinning techniques and Mansfield (6) has presented within a general review a discussion of dipolar

echo phenomena. The monograph by Goldman (10) has discussed the thermodynamics of spin systems in solids, while spin-lattice relaxation in solids has been the subject of a number of reviews (11-15). A number of current articles (16-27) are furnishing an improved understanding of relaxation in the presence of rf irradiation.

The present article will not discuss the experimental aspects of using the high-resolution, solid state techniques. In general, they require the use of Fourier-transform techniques and have depended heavily on the development of solid state radio-frequency components to allow both the application of high-power rf-pulse trains and the reception of microvolt-level NMR signals in the presence of such irradiation. Several homebuilt spectrometers have been described in detail (28-30), and theoretical criteria for design of multiple-pulse spectrometers have been presented (31). The recent introduction of commercial instrumentation capable of performing these kinds of measurements may aid in reducing the difficulties encountered by one entering the field.

As mentioned above, the main focus of this article will be to describe and evaluate recently developed experiments which offer promise of usefulness

in dealing with complex materials.

As these experiments tend to deal with several of the solid state Hamiltonians simultaneously, we will first review each of the Hamiltonians of interest separately. This will include a description of the means which have been developed to control the effective form of that particular Hamiltonian and how these experimental schemes have been used. The latter sections will then discuss several specific experiments illustrating the capabilities of these more complex spectroscopic experiments.

#### BACKGROUND

An isolated nucleus of spin  $I$  placed in a magnetic field will have  $2I + 1$  equally spaced energy levels. If, however, the nucleus is not isolated but interacts with surrounding nuclei and electrons, these energy levels can be shifted and split (7,8), and measurement of these perturbations furnishes information on the physical and chemical environment of the nucleus. The Hamiltonian,  $H$ , of the nucleus thus consists of several components, for example:

$$H = H_z + H_Q + H_D^{II} + H_D^{IS} + H_\sigma + H_{etc} + H_{rf}^{(t)} \quad (1)$$

where:

$H_Z$  = Zeeman Hamiltonian due to presence of the large static magnetic field.

$H_Q$  = quadrupolar Hamiltonian which can be present for  $I > \frac{1}{2}$  and furnishes information on the electric field gradient at the nuclear site.

$H_D^{II}$  = homonuclear dipolar Hamiltonian resulting from direct dipole-dipole interactions between like nuclei which furnishes molecular-level geometrical information on the relative location of the nuclei.

$H_D^{IS}$  = heteronuclear dipolar Hamiltonian resulting from direct dipole-dipole interactions between unlike nuclei which furnishes molecular-level geometrical information on the relative location of the interacting nuclei.

$H_\sigma$  = chemical-shift Hamiltonian due to the shielding produced at a nuclear site by motion of charged particles, primarily electronic orbital motion.

$H_{etc}$  = all other interactions which may be present but will not be of interest in the present article; particularly note that this term includes effects of electron spin-nuclear spin interactions and

higher-order (electron-coupled) nuclear spin-spin interactions (7,8).

and finally:

$H_{rt}^{(t)}$  = the applied radio-frequency fields which are used to produce the macroscopic magnetization experimentally observed and to provide a means to control the effect other Hamiltonians have on the time development of the macroscopic magnetization.

For the experimental conditions to be considered here, the Zeeman Hamiltonian,  $H_z$ , will always be much larger than any of the other interactions present, and one needs to consider only the portion of the other Hamiltonians which remain time independent in the presence of a large Zeeman interaction. That is, one needs to consider only the secular portions of each of the remaining Hamiltonians. It will be the practice here to discuss such Hamiltonians in the rotating frame of reference, i.e., in the interaction frame of the Zeeman Hamiltonian (7,8).

Each of these Hamiltonians contains information about the physical or chemical environment of the nuclei under study, and in addition to being orientationally dependent, each of these Hamiltonians will be altered in characteristic ways by molecular motion depending on the

frequency and anisotropic nature of the motional phenomena. There is, thus, a large amount of information potentially available from these interactions, and yet it has been possible in the past to extract only a small portion in a useful form. Past difficulties have involved situations where one interaction was so large that it obscured other terms or where several terms were of nearly equal size; thus, quantitative characterization of the individual terms proved difficult. In general, the extensive orientational information potentially available from these anisotropic interactions has been lost when dealing with polycrystalline samples.

The realization that there were steps of an experimental nature which one could take to resolve these difficulties has resulted in the development of the high-resolution, solid state NMR techniques. These schemes involve the application of a perturbation to the system to alter in a fundamental way how the system will be affected by a particular Hamiltonian. That is, one does not have to accept the set of Hamiltonians as given in Equation 1 as unalterable but can devise perturbations which, when applied to such a system, will amplify or suppress the effects of a particular interaction to allow the experimental characterization of the

individual Hamiltonians. It is now possible to obtain a detailed quantitative characterization of the several interactions terms by performing a series of measurements using different perturbations, and recently, it has been demonstrated that one can use two perturbations consecutively in a single experiment to correlate two interaction terms. This correlation of the action of two Hamiltonians is valuable particularly for extracting detailed orientational information in polycrystalline samples. That is, each of the Hamiltonians discussed above has a strong angular dependence, and in experiments on a polycrystalline sample where one such Hamiltonian is singled out, one, in general, obtains a powder pattern from which the magnitude and some general structure for the angular dependence of the Hamiltonian is obtainable. However, it is not possible in such experiments to obtain the detailed orientational information obtainable from experiments performed on a single crystal as a function of its orientation. By modulating the effects of one Hamiltonian on a second, however, one produces essentially two-dimensional spectra from which the detailed orientational information from one Hamiltonian is correlated with the orientational dependence of the second Hamiltonian, and this allows one to extract

more information than would be available from conventional experiments performed on a single crystal. This point is more easily appreciated with the aid of concrete examples and several will be discussed in detail below. First, however, a brief description of each of the Hamiltonians indicated in Equation 1 will be presented with a summary of the means which have been developed to modify and control its form.

#### The Dipolar Hamiltonians

A direct nuclear dipole-nuclear dipole interaction occurs between nuclei with nonvanishing magnetic moments. The Hamiltonian for such interactions in the presence of a strong static magnetic field is indicated below where only the geometrical terms are given explicitly.

$$H_d \propto \sum_{ij} (1 - 3 \cos^2 \theta_{ij}) / r_{ij}^3 \times (\text{spin function}) \quad (2)$$

" $\theta_{ij}$ " is the angle between the external magnetic field direction and the internuclear vector joining the two interacting nuclei and " $r_{ij}$ " is the internuclear distance. One notes that this interaction is a strong function of the relative positions of the nuclei and thus may be used to obtain geometrical, really molecular-frame, information on the location of nuclei in solids. Additionally, since motion of nucleus,  $i$ , relative to nucleus,  $j$ ,

allows  $H_d$  to become time dependent and can alter the observed spectrum, the dipolar interaction is used to investigate motional phenomena (diffusion, internal reorientation, etc.) in solids. Studies using the direct dipolar coupling to obtain geometrical and motional information have a long history, starting essentially with the initial applications of NMR to solids, and constitute a major fraction of presently reported solid state NMR studies.

In the past much of the detailed information contained within this Hamiltonian has been lost except for studies of materials where the natural occurrence of a small number of spins in isolated groups produced a relatively simple Hamiltonian (7,8). Complexities due to additional nearby interacting nuclei cause a severe complication of the spectra, and the presence of large homonuclear interactions can prevent the observation of the details of any heteronuclear interactions present simultaneously. In addition, the orientation dependence of the dipolar interaction results in a smearing in spectra from polycrystalline samples, and with conventional wideline techniques one normally only obtained a single parameter (the second moment) to characterize the geometry.

A number of the solid state NMR techniques developed in recent years

have involved methods to alter the nature of the dipolar interactions. The earliest efforts involved the use of rapid sample rotation with the rotation axis tilted at the "magic angle" of  $54^{\circ}44'$  to the external magnetic field (5,32,33). Such magic-angle sample-spinning techniques have been of limited utility for removal of dipolar broadening to date, however, since the rotation rates required proved technically difficult to obtain in many situations. Also, the fact that one removed the anisotropy in the chemical shift tensors reduced the usefulness of the technique. (As it turns out, such magic-angle sample-spinning is proving very useful for simplifying chemical shift spectra in complex materials as will be discussed below.)

The more recent development of multiple-pulse techniques (1,2) for suppression of homonuclear dipolar broadening has allowed the widespread measurement of chemical shift tensors of an abundant spin in solids. Likewise, the suppression of heteronuclear dipolar interactions by a strong resonant irradiation of an abundant, I, species furnishes a means to measure other interactions of a dilute, S, species. However, measurement of the chemical shift tensors of a dilute spin species only became widespread after the development of means to enhance the signal-to-noise of the spectra. Both direct (30)

and indirect (34-36) schemes for dilute spin signal enhancement have been demonstrated which involve transfer of polarization between the abundant and dilute spins (37) coupled by the heteronuclear dipolar interaction. The direct scheme has seen widespread use, particularly for measurement of  $^{13}\text{C}$  chemical shift tensors (1). An understanding of the dynamics of spin systems coupled with inhomogeneous dipolar interactions and subject to intense rf decoupling fields is beginning to appear (38-42).

In closing this brief discussion of the dipolar Hamiltonians, it should be noted that the interpretation of the dipolar Hamiltonian to furnish structural information on the scale of a few Å (basically near- and next-neighbor geometry) is rigorous and does not require any form of empirical correlation. The only complicating factor is the possibility that an indirect coupling between the nuclear spins through the electronic states (7,8) could occur and thus distort the experimentally measured dipolar Hamiltonian. There is, however, no direct evidence for such distortions in measurements reported to date of the lighter nuclei,  $^1\text{H}$ ,  $^2\text{H}$ ,  $^{13}\text{C}$ , or  $^{14}\text{N}$ .

#### The Chemical Shift Hamiltonian

The electron distribution surrounding a nucleus will distort slightly

both the magnitude and direction of the applied magnetic field,  $\vec{H}_0$ , to produce an effective field at the nuclear site,  $\vec{H}'$  (7,8). Consequently, the Hamiltonian for the interaction of the external field with the magnetic moment of the nucleus,  $\vec{\mu}$ , involves a shielding tensor,  $\vec{\sigma}$ .

$$H_{\sigma} = \vec{\mu} \cdot \vec{H}' = \vec{\mu} \cdot (1 - \vec{\sigma}) \cdot \vec{H}_0 \quad (3)$$

Essentially,  $\vec{\sigma}_i$  is a magnetic shielding tensor, but since it is a function of the electronic environment and its study furnishes information on chemical bonding, it is labeled the chemical shift tensor.

In general, nine independent quantities are needed to specify a second-rank Cartesian tensor such as the chemical shift tensor. However, only the symmetric part of the chemical shift tensor affects the spectra in first order with the large magnetic fields typically used in NMR studies; consequently, one is only interested in the six quantities needed to specify the symmetric portion of the chemical shift tensor. The six quantities, normally presented as the three principal values and the three angles needed to specify the orientation of the principal axis system, can be obtained by observing the resonance position in a single crystal as a function of orientation.

Additionally, it is possible to determine the three principal values from a

polycrystalline powder spectrum.

Routine measurement of chemical shift tensors in solids has only become possible in recent years with the development of the high-resolution, solid state NMR techniques since normally the chemical shift interaction is smaller than dipolar interactions present, and unless some means to remove the effect of the dipolar interactions is available, the smaller chemical shift interaction is masked. Means for suppressing both homonuclear and heteronuclear dipolar interactions for spin  $\frac{1}{2}$  nuclei have developed and are in widespread use for measurements of chemical shift tensors (1,2,43-55) and still other schemes are being suggested (56). In addition, double quantum schemes have recently been demonstrated (57-60) which both eliminate first-order quadrupolar interactions and furnish means to suppress heteronuclear dipolar interactions. Finally, experimental methods to determine accurately the center of mass of a dipolar-broadened line can furnish chemical shift information in special cases (61-65).

In liquids where rapid molecular motion removes the effects of the dipolar coupling from NMR spectra, chemical shift measurements have been extensively used to investigate a wide variety of phenomena. The

molecular motion averages the chemical shift tensor so that all that can be measured directly in a liquid is the average, or trace, of the chemical shift tensor. However, measurement of even the trace of the chemical shift tensor has proven highly informative, and knowledge of the full tensor furnishes a much greater amount of detailed information on the geometry and electronic structure, or chemical bonding, within the investigated material. For example, the nonspherical nature of the electronic distributions around atoms involved in chemical bonding is directly indicated by the differences between the three principal values of the chemical shift tensor, while knowledge of the trace of the tensor means one can only indirectly infer information on such anisotropy. Theoretical efforts to interpret the chemical shift tensor by first-principle calculations are not impressive at present (1,2,43,44); however, the sensitivity of the chemical shift tensor to even small changes in electronic environment has been experimentally demonstrated. In addition, the geometrical nature of the chemical shift tensor makes it a useful probe for detecting and characterizing motional phenomena within solids, particularly anisotropic motional phenomena (1). The use of the chemical shift tensor in investigation of

the properties of solid materials is still in its infancy with the bulk of work done to date involving primarily the measurement and cataloging of information of model systems (1,2,43-55). However, applications have begun to appear, for example: examination of solid state phase changes (66,67), characterization of polymers (68-73), solid hydrocarbon fuels (74-77), heterogeneous catalysts (78-80), and biological materials (81-83).

#### The Quadrupolar Hamiltonian

The quadrupolar Hamiltonian furnishes information on the electric field gradient ( $V_{ij}$ ) at the nuclear site (7,8). Written in the principal axis frame of  $V_{ij}$ , the quadrupole Hamiltonian is:

$$H_Q = \frac{e^2 Qq}{4I(I-1)} [3I_z^2 - I^2 + \eta(I_x^2 - I_y^2)] \quad (4)$$

where,

$$eq = V_{zz} \quad (V_{zz} \text{ is defined as the larger of the } V_{ii} \text{'s})$$

$$\eta = (V_{xx} - V_{yy}) / V_{zz}$$

$Q$  = quadrupolar moment of nucleus with spin  $I$

Since we are interested in the case where the quadrupole Hamiltonian serves as a perturbation on a larger Zeeman interaction, we must consider explicitly the orientation of the principal axis of the electric field gradient in the laboratory reference frame in calculating the perturbation energies (9,84). Using the standard Euler angles  $(\theta, \phi, \gamma)$  (85), one obtains for both first-order,  $\Delta E_Q^1$ , and second-order  $\Delta E_Q^2$ , energy shifts:

$$\Delta E_Q^1 = (h\nu_Q/4) (3 \cos^2\theta - 1 - \eta \cos 2\alpha \sin^2\theta) (m^2 - I(I+1)/3) \quad (5)$$

$$\begin{aligned} \Delta E_Q^2 = \frac{h\nu_Q^2 m}{48\nu_Z} & \left[ \frac{3}{2} \sin^2\theta \{ \cos^2\theta [34m^2 + 5 - 18I(I+1)] - 2m^2 - 1 + 2I(I+1) \} \right. \\ & + \eta \cos^2\phi \sin^2\theta \{ \cos^2\theta [34m^2 + 5 - 18I(I+1)] + 2m^2 + 1 - 2I(I+1) \} \\ & + \frac{\eta^2}{6} \{ 4(8m^2 + 1 - 4I(I+1)) - 4 \cos^2\theta [5m^2 + 1 - 3I(I+1)] \\ & \left. - \cos^2 2\theta (\cos^2\theta - 1)^2 [34m^2 + 5 - 18I(I+1)] \} \right] \quad (6) \end{aligned}$$

where:

$$\nu_Q = \frac{3e^2 q Q}{2I(I-1)\hbar}$$

$$\nu_Z = \text{Zeeman splitting} = \gamma H_0 / 2\pi$$

The quadrupolar Hamiltonian can be large enough that the second-order energy shifts are comparable with other terms considered above, i.e., chemical

shifts and dipolar splittings, and thus both first- and second-order effects must be considered.

Suppression of the quadrupolar Hamiltonian can present additional problems, particularly when it is large. In cases where the quadrupolar splittings are small,  $\lesssim 50$  kHz, the second-order effects can be ignored and one can remove the first-order effects with the same multiple pulse techniques used for suppression of homonuclear dipolar broadening (1,86). When the quadrupole splittings grow large, one can resort to use of multiple quantum transitions between levels which are shifted the same amount by the first-order quadrupolar effects (57-60, 87-89). Results for a spin 1 system, deuterium, have demonstrated suppression of heteronuclear dipolar interactions between two nuclei, one of which is badly quadrupolar broadened (57,60) by stirring the system with double quantum transitions. In addition, high-resolution deuterium spectra (i.e., without first-order quadrupolar broadening) have also been obtained by monitoring the time development of the off-diagonal, double quantum density matrix element (58,60). Moreover, it should be remembered that for nuclei with nonintegral spin the  $\frac{1}{2} \leftrightarrow -\frac{1}{2}$  transition will not be affected by first-order quadrupolar broadening. Thus, several methods

are available for suppressing the effects of quadrupolar broadening.

A second aspect of control of the quadrupolar Hamiltonian is developing means for its characterization. Since the quadrupolar Hamiltonian is, in many cases, the largest interaction present except for the Zeeman, it can be observed directly in many cases, (90,91) for example. Recently, heteronuclear dipolar decoupling together with spin dilution techniques have been used to enhance the resolution available for quadrupolar measurements in single crystals (92,93). A major difficulty with nuclei with larger quadrupolar moments is that the distribution of electric-field gradients present can broaden the line to the point that it cannot be detected (9,84). In such cases, for nuclei with nonintegral spin, it has been possible to observe the  $\frac{1}{2} \leftrightarrow -\frac{1}{2}$  transition and extract information from the second-order effects on this transition. Recently (94), an interferometric spectroscopic technique used initially for a demonstration of spinor character (95) has been developed to allow detection of first-order quadrupolar satellite spectra from observation of only the central  $\frac{1}{2} \leftrightarrow -\frac{1}{2}$  transition. This scheme not only allows a direct determination of broad first-order quadrupolar spectra, but allows a correlation of first- and second-order quadrupolar

energy shifts (94), i.e., a two-dimensional map, which should be of value in complex solids, such as the beta-alumina examined, where there are multiple inequivalent nuclear sites and anisotropic motional processes exist.

#### MORE COMPLEX CHARACTERIZATION SCHEMES

The brief review of each of the several interactions considered above indicates the complexity of the developing high-resolution, solid state NMR techniques as well as their potential for furnishing information. However, even more detailed information can now be obtained at the expense of additional complexity. That is, by applying more than one method of modifying the Hamiltonians simultaneously or sequentially, one can further enhance the information content of the experimental data. Even though these more complex experiments are still in the developmental stages, the three examples discussed below will clearly demonstrate that they greatly enhance the information available. It should be remembered that these are examples of the type of experiment now possible and that they are not to be considered as an inclusive list.

#### Sample Spinning; Chemical Shifts

As discussed in some detail above, the removal of dipolar broadening

has allowed measurement of the chemical shift tensor for a variety of nuclei in the solid state. Spectra obtained from polycrystalline samples of all but the most simple materials can exhibit complex spectra as the chemical shift powder patterns of chemically inequivalent nuclei are normally sufficiently broad to overlap, and an analysis of such a group of overlapping powder patterns is difficult. Such spectra can be simplified if one will physically spin the sample (32,33) as well as simultaneously apply radio-frequency irradiation to remove the dipolar broadening (96). A rotation of a sample with the sample rotation axis at an angle of  $54^{\circ}44'$  (the magic angle) to the static magnetic field,  $H_0$ , will cause an averaging of the chemical shift tensor, and if the rotation is rapid compared to the inverse width of the chemical shift powder pattern for a particular nuclei, the chemical shift powder pattern collapses to a single line at the average, or one-third of the trace, value of the chemical shift tensor. Thus, overlapping powder patterns become a series of sharp lines whose amplitudes and frequencies are easily determined (71,96). Figure 1, taken from the work of Schaefer, Stejskal and Buchdahl (69), illustrates the effect of combined heteronuclear decoupling and rapid sample spinning at the magic angle on the  $^{13}\text{C}$  spectra

of a polycarbonate polymer sample.

This procedure can simplify complex spectra and is sufficient to allow classification of the various chemical environments of an observed nuclei and a determination of their relative concentrations, thus providing an analytical characterization of complex solids very similar to that available for molecules in solution by conventional NMR. In addition, once isolated lines corresponding to chemically inequivalent species are obtained, it is possible to measure other parameters such as their relaxation behavior and further characterize the various species present (69).

By this procedure, however, one loses information on the anisotropy in the chemical shift tensors, i.e., one has the trace value but not the individual principal values of the chemical shift tensor. Again, however, an additional complication of the experimental procedure will allow one to keep the simplicity of the collapsed spectra and retrieve knowledge of the principal values of the individual chemical shift tensors. Several schemes for doing this have been reported recently, ranging from simply moving the angle of sample rotation off the magic angle by a few degrees or slowing the spinning rate to less than the inverse width of the individual powder

patterns (97,98) to more complex two-dimensional schemes involving  
rf irradiation (97-99). More recently, data sampling with a variable  
in synchronization with the slow sample rotation (100) has been shown  
as a means to retrieve the individual chemical shift tensor principal

A tilting of the sample spinning axis off the magic angle results in a  
scaled powder pattern, and one can scale the powder patterns with their  
trace values to the point that they no longer overlap and thus obtain  
scaled powder patterns to determine the principal values of each  
shift tensor. A slowing of the sample spinning rate to below the  
width of the powder pattern but maintaining the spinning rate above  
homogeneous linewidth of an individual nuclei will result in the  
of a group of sidebands whose relative amplitude depends on the anisotropy  
in the chemical shift tensors (97). Figure 2, taken from the work of  
Stejskal, Schaefer, and McKay (98) illustrates the effects of both  
spinning and spinning off-angle on a  $^{13}\text{C}$  spectra of a polycarbonate  
sample. Figure 1 illustrates the effects of rapid sample spinning  
magic angle on a similar polycarbonate polymer sample, and the comparison  
to the spectra produced by off-angle spinning and by slow spinning

visible in comparing the two figures. It has been suggested (98) that the off-angle spinning scheme offers more difficulties in interpretation since one still is likely to have overlapping powder patterns that must be separated, possibly by several choices of the spinning angle, while it is only necessary to know the spinning rate to assign the sidebands in the slow-spinning case. Figure 3 illustrates the relationship between the sideband intensities and the tensor anisotropy for a simpler case, the  $^{31}\text{P}$  spectra of barium diethylphosphate (BDEP) here the mapping out of the tensor by the sideband intensities is clearly evident (101).

Numerous sample-spinning experiments have been reported in the past two years, both with simultaneous suppression of homonuclear dipolar interactions (102,103) and observation of the abundant spin as well as simultaneous suppression of heteronuclear dipolar interactions (69-71, 74,77,96-98,100, 101,104-106) and observation of a dilute spin. Quite complex solids including polymeric materials (69-71), solid hydrocarbons (74,77), and biological membranes (104) have been examined, and both the cause of residual linewidths (105) and the details of cross-polarization under sample-spinning conditions (106) have been discussed. To date, only chemical shift powder patterns have

been examined with these schemes; however, any inhomogeneously broadened line could be treated similarly, and it has been suggested that heteronuclear dipolar interactions (with the abundant spin homonuclear dipolar interaction suppressed) (96) and first-order quadrupolar interactions (100) could be treated profitably.

#### Correlation of Dipolar and Chemical Shift Hamiltonians

It has been one of the frustrations of solid state NMR that the strong orientational dependence of many of the Hamiltonians which inherently can furnish a wealth of detailed information has tended instead to reduce the information content of solid state NMR spectra, particularly when dealing with polycrystalline systems. The strong anisotropies present have tended to broaden and smear spectra from polycrystalline samples and reduce the information that could be obtained. The initial section of this review discussed the various means which have been developed to control the effective form of the various Hamiltonians, primarily so that one could experimentally sort and characterize the individual interactions present. It is the purpose of this section to illustrate that in addition to simply characterizing a single Hamiltonian, one can, by a careful choice of experiment, correlate

or modulate one anisotropic interaction upon another in such a way as to extract much of the orientational information present in both Hamiltonians. Such schemes depend upon an experimental ability to change the nature of the time development of a spin system part way through an experiment. That is, if the spin system is allowed to evolve under the direction of, first, one effective Hamiltonian and then a second effective Hamiltonian during a single evolutionary period, the observable magnetism will carry information on both Hamiltonians. Since there are two independent variables, one can obtain a two-dimensional presentation of the results by repeating the experiment sufficiently to collect a matrix of observations (i.e., observable as a function of both evolutionary times,  $t_1$  and  $t_2$ ). Such a two-dimensional matrix can be analyzed to furnish more information than simply performing experiments involving each of the two Hamiltonians separately and, as will be illustrated below, can offer a very great advantage in many cases. The analysis of the data could be performed in the dual-time domains, but normally it is found convenient to Fourier-transform to a mixed time-frequency domain or a dual-frequency domain. The examples illustrated below will illustrate the mixed-domain analysis (107-108), and the dual-frequency-

domain analysis has been formalized and discussed in detail within the context of conventional high-resolution NMR of liquids (109-111) and used in solid state studies (112-114).

Since much of the effort that has gone into the development of high-resolution solid state NMR techniques has been directed to developing means to alter the nature of the effective Hamiltonian controlling the time development of a spin system, it is only necessary to combine two such control schemes within a single experiment. This can be illustrated particularly well by a correlation of the dipolar and chemical shift Hamiltonians. The dipolar Hamiltonian contains information on the local molecular geometry around a nuclear site (bond angles and distances), while the chemical shift Hamiltonian characterizes the electronic structure or chemical bonding near a nuclear site; thus, a correlation of these Hamiltonians can both allow one to (i) orient the chemical shift tensor in the local molecular frame and (ii) determine the geometry of the local molecular frame (bond distances and relative bond angles).

The simplest situation occurs in the case of a single crystal, or highly oriented material, where substantial dipolar structure exists because

of a clustering of spins, i.e.,  $^{13}\text{CH}_2$ ,  $^{13}\text{CH}_3$ ,  $\text{H}_2\text{O}$ ,  $\text{SH}_2$ , etc., and one can take free induction decay spectra as a function of orientation and assign the dipolar multiples (48,93). Additionally, by suppressing the abundant spin dipolar interactions, one could observe the direct dipolar interactions between dilute spin species (72,115) in a similar fashion. The more complex situation occurs when the dipolar structure is apparently lost due to the unoriented nature of the sample, and it is this case which will be treated in detail below.

#### HETERONUCLEAR DIPOLAR VS. DILUTE-SPIN CHEMICAL SHIFT HAMILTONIAN

The initial dipolar chemical-shift-correlated experiments evolved from the dilute-spin double resonance schemes of Pines et al (30) since these experiments used two evolutionary periods to begin with, although in a less general fashion. The initial step in the dilute spin double resonance experiment was to produce a dilute spin (S-spin) polarization by transferring polarization through the heteronuclear dipolar Hamiltonian from the abundant spin (I-spin), and then the S-spin polarization was observed during a second time period as it evolved under the chemical shift Hamiltonian. While these experiments were normally performed with a fixed cross-polarization period

chosen to optimize signal-to-noise, by collecting data as a function of the evolution under the chemical shift Hamiltonian,  $t_2$ , for a variety of cross-polarization times,  $t_1$ , a two-dimensional data matrix of the type discussed above could be collected. Muller et al (116) reported oscillations in the cross-polarization as a function of cross-polarization times in a single crystal of ferrocene, and VanderHart (55) has used cross-polarization rates to determine the molecular frame orientation of a methylene  $^{13}\text{C}$  chemical shift tensor. Since resolution of the heteronuclear dipolar interaction in such experiments would be expected to be hindered by the presence of a large homonuclear dipolar interaction present between the abundant species, I, the next step was development of schemes to allow the cross-polarization to proceed while suppressing simultaneously the homonuclear dipolar interaction between the abundant spins. Hester et al (117) accomplished this by cross-polarizing with continuous off-resonance irradiation, which satisfied the Lee-Goldberg criteria (118) for suppression of homonuclear dipolar interactions, while Stoll et al (119) later devised and demonstrated a multiple-pulse scheme for simultaneous transfer of polarization and suppression of homonuclear dipolar interactions. A final step in the evolution of this techniques, taken simultaneously by

these two research groups (107,112), was to change the two-evolutionary-period experiment into a three-evolutionary-period experiment by: (i) returning the cross-polarization period to its original purpose of creating a large dilute-spin transverse magnetism, (ii) adding a period in which conventional heteronuclear dipolar interaction (equivalent to an AX case of spin-spin coupling) takes place (for time  $t_1$ ) with a multiple-pulse sequence used to suppress homonuclear dipolar broadening, and (iii) maintaining the final evolutionary period ( $t_2$ ) in which the chemical shift Hamiltonian controlled the evolution of the dilute spin. This form of the experiment proved technically easier to perform, and the results are more straightforward to analyze. The experiment of Stoll et al (107-108) also refocused the chemical shift development occurring during the dipolar evolutionary period and is, thus, more applicable to polycrystalline systems and will be discussed below as a prototype example of these still-developing schemes.

Figure 4A illustrates the pulse sequence used for these dipolar-modulated chemical shift experiments (107). During the initial period a Hartmann-Hahn (37) transfer of polarization takes place from the I-spins

to the S-spins in order to produce a large observable transverse S-polarization. During the second period, the S-spin polarization evolves under both chemical shift ( $H_{OS}^0$ ) and I-S heteronuclear dipolar interaction ( $H_{IS}^0$ ), with I-I homonuclear dipolar interactions suppressed using an eight-pulse cycle (31). That is:

$$\overline{H}_S = \overline{H_{OS}^{(0)}} + \overline{H_{IS}^{(0)}} \quad (7)$$

where

$$\overline{H_{OS}^{(0)}} = \sum_j (\Delta\omega + \omega_0\sigma_{zzj}) S_{zj}, \quad (8)$$

$$\overline{H_{IS}^{(0)}} = \sum_i \sum_j \frac{\alpha B_{ij}}{3} (I_{zi} + I_{xi}) S_{zj} \quad (9)$$

with

$$B_{ij} = (\gamma_i\gamma_j\hbar/r_{ij}^3) (1 - 3\cos^2\theta_{ij}) \quad (10)$$

At the end of this evolutionary period ( $t_1$ ), the eight-pulse cycle is replaced with a strong resonant decoupling field on the I-spin system to halt the time development of the heteronuclear dipolar interaction but allow the chemical shift and off-resonance Hamiltonian of the S-spin system to continue controlling the evolution of the S-spin system. In order to recover the initial part of the S-spin chemical shift evolution, a  $180^\circ$  refocusing pulse

(Carr-Purcell-Meiboom-Gill type) is applied to the S-spin system, and the second half of the S-spin system echo is recorded digitally to furnish one set of data (i.e., a set of amplitudes as a function of  $t_2$  for a given  $t_1$ ). Since the heteronuclear dipolar and chemical shift Hamiltonians controlling the S-spin system during the initial evolutionary period,  $t_1$ , commute, the refocusing pulse separates the evolution of the S-spin system under the dipolar Hamiltonian from the evolution under the chemical shift Hamiltonian. Thus, while one could use double-transform techniques on a full matrix of data as a function of  $t_1$  and  $t_2$ , it proves simpler to consider the dipolar-modulated chemical shift spectra individually. That is, one produces individual chemical shift spectra for the S-spins in which all of the effects of the heteronuclear dipolar evolution appear as an initial simple modulation by performing the experiment for a single  $t_1$  and then transforming the digitally recorded echo. The time development of S-magnetization is, for example:

$$\langle S_x \rangle \propto \sum_j (\sin (\sigma_{jzz}\omega_0 + \Delta\omega) t_2) \prod_i \cos(\alpha\beta_{ij}t_1/3\sqrt{2}) \quad (11)$$

$$\langle S_y \rangle \propto \sum_j (\cos (\sigma_{jzz}\omega_0 + \Delta\omega) t_2) \prod_i \cos(\alpha\beta_{ij}t_1/3\sqrt{2}) \quad (12)$$

A Fourier-transform over the echo,  $t_2$ , for a given  $t_1$  will produce powder patterns for the S-spin system, with the initial amplitudes for each S-spin

modulated by a dipolar evolution for time,  $t_1$ . Figures 5 and 6 exhibit both theoretical and experimental dipolar-modulated chemical shift powder patterns for  $^{13}\text{C}$  in solid benzene in its rotator phase at  $-90^\circ\text{C}$ .

The individually calculated dipolar-modulated spectra are stacked in Figure 5 to produce the type of mixed,  $t_1$  by  $\omega_2$ , presentation discussed above, and they are individually compared to the experimental data in Figure 6. The local nature of the molecular-frame information obtained is illustrated with the theoretical results presented in Figure 5, where the results presented in Figure 5A were obtained considering only the dipolar interaction between the  $^{13}\text{C}$  and its directly bonded proton, while the results presented in Figure 5B were calculated considering other nearby protons as well (particularly the two protons directly bonded to carbon, which are nearest neighbors to the  $^{13}\text{C}$  since they are only approximately  $2 \text{ \AA}$  from the  $^{13}\text{C}$ ). One observes that all gross features are controlled by the directly bonded protons, while those farther out tend primarily to dampen out the dipolar oscillations produced by the directly bonded  $^1\text{H}$ - $^{13}\text{C}$  dipolar interaction. In Figure 6, a direct comparison is made between the experimental spectra and the calculation of Figure 5B with only every other spectrum of Figure 5B

presented in Figure 6; that is, 100 microsecond intervals of  $t_1$  are used in Figure 6, while in Figure 5 each spectrum corresponds to 50 microseconds of additional dipolar evolution. One notes the experimental data correspond closely to what was calculated considering the other protons in the benzene molecule, but they do not correspond to the spectra calculated considering only the directly bonded protons at times greater than 150 microseconds. (See Figure 4 of reference 107 for a comparison between the calculation for the single  $^{13}\text{C}$ -proton case and the experimental data.) Another feature used to analyze these spectra is to consider the areas of the spectra as a function of the dipolar evolution time,  $t_1$ . The expression for the relative area as a function of  $t_1$  is independent of the orientation of the chemical shift tensor in the molecular frame (107,108) although the shape is clearly strongly dependent on such orientation. The relative area is an integral over the  $4\pi$  solid angle of a product of the dipolar modulation terms (108):

$$\frac{A(t_1)}{A(0)} = \frac{1}{4\pi} \int \prod_i \left[ \cos \left( \frac{\alpha t_1 B_{i1}}{3\sqrt{2}} \right) \right] d\Omega \quad (13)$$

where the index,  $i$ , is over protons near the  $^{13}\text{C}$ . Thus, for example, the  $^1\text{H}$ - $^{13}\text{C}$  bond distance can be determined from the areas of the dipolar-modulated chemical shift spectra alone.

## HOMONUCLEAR DIPOLAR VS. ABUNDANT-SPIN CHEMICAL SHIFT HAMILTONIAN

The modulation, or correlation, of the chemical shift Hamiltonian with the dipolar Hamiltonian has a number of advantages, as have been discussed above, and another quite different, and yet similar, example (108) will be discussed to emphasize both the generality and capability of these experiments.

In addition to the situation discussed above in which one has a dilute spin interacting with members of an abundant-spin system, there are many cases in which the members of an abundant-spin system are not uniformly dispersed within a solid but occur within relatively isolated complexes (i.e., for  $^1\text{H}$ , for example,  $-\text{CH}_2$  or  $\text{H}_2\text{O}$  groups), and thus structure exists in the homonuclear dipolar Hamiltonian due to strong dipolar interactions within such a group compared to the much weaker interactions between groups. Thus, one would like to modulate this homonuclear dipolar interaction upon the abundant-spin chemical shift powder pattern. The pulse sequence necessary to produce a homonuclear dipolar-modulated chemical shift spectra in this case is illustrated in Figure 4B, where it can be compared to the heteronuclear dipolar-modulated case of the dilute spin in Figure 4A.

Since only a single abundant-spin species, I, is involved, irradiation is needed at a single frequency. First, an observable transverse I-spin magnetization is produced with a  $90^0$  pulse; the system is allowed to evolve under a combination of chemical shift and homonuclear dipolar Hamiltonians for a period,  $t_1$ ; and then an eight-pulse cycle effective in suppressing homonuclear dipolar interactions (31) is applied (at  $t_2 = 0$ ), and the system continues to evolve under an effective chemical shift Hamiltonian (31). If one stroboscopically samples the magnetization at the appropriate window in the eight-pulse sequence during the evolutionary period,  $t_2$ , the data collected can be Fourier-transformed to produce a homonuclear dipolar-modulated chemical shift spectrum. A pulse to refocus the chemical shift time development during evolutionary period,  $t_1$ , has not been shown here since it may not always be desirable (particularly if the intense localized homonuclear dipolar term will not commute with the chemical shift Hamiltonian). In any case such a refocusing pulse would be placed at  $t_1/2$  since the effective rotation axis for the chemical shift Hamiltonian is different with and without the eight-pulse cycle (31).

This sequence was initially demonstrated on the protons in  $\text{CCl}_3\text{COOH}$  (108).

Trichloroacetic acid dimerizes in the solid state to produce relatively isolated pairs of protons within dimerized carboxylic groups, while the chlorine groups decouple themselves. The Hamiltonian for the evolution period,  $t_1$ , for the proton pair is:

$$H(t_1) = \frac{\gamma_H^2}{2r_{12}^3} (1 - 3 \cos^2 \theta_{12}) (3I_{z1} I_{z2} - \vec{I}_1 \cdot \vec{I}_2) + H_D (\text{inner}) \\ + (\Delta\omega + \sigma_{zz1}) I_{z1} + (\Delta\omega + \sigma_{zz2}) I_{z2}$$

where  $\theta_{12}$  is the angle between the vector joining the two protons and the direction of the external magnetic field;  $\sigma_{zz1} = \sigma_{zz2}$  by symmetry for the two protons in the system; and  $H_D (\text{inner})$  is the portion of the dipolar Hamiltonian that couples the proton pair with the other proton pairs in the system.  $H_D (\text{inner})$  is small enough to be ignored here (108), and the remaining terms of the Hamiltonian commute so one could use a refocusing pulse. During the evolution period,  $t_2$ , the effective Hamiltonian takes the form:

$$H(t_2) = \frac{\alpha}{3} [(\Delta\omega + \sigma_{zz1}) (I_{x1} + I_{z1}) + (\Delta\omega + \sigma_{zz2}) (I_{x2} + I_{z2})] + \text{(higher-order terms)}$$

where  $\alpha$  is a correction factor accounting for the finite-pulse width. Figure 7 illustrates the proton spectra obtained, and one notes that for the longest dipolar evolution time used,  $t_1 = \sim 300$  microseconds,

well-resolved spectrum is obtained confirming the small size of  $H_D$  (inner). These spectra can be treated in a fashion similar to the heteronuclear dipolar-modulated chemical shift spectra discussed above, and one can determine both the length of the proton-proton vector and its orientation within the proton chemical shift tensor principal-axis frame by least-square fitting the spectra. Such theoretical fits to selected spectra are exhibited in Figure 8. Since only one molecular-frame vector, the proton-proton vector, is present in this case, the location of the chemical shift tensor principal-axis frame in the molecular frame can be determined to within a single arbitrary rotation around this proton-proton vector. Single-crystal rotation studies had previously been performed on trichloroacetic acid and, due to ambiguities produced by the existence of multiple sites, had produced two possible orientations for the chemical shift principal-axis frame (48). The present polycrystalline study is able to orient the chemical to within a single rotation, and the combination of the results of the two experiments furnishes a unique orientation for the proton chemical shift tensor in the molecular frame of reference. Thus, not only can one determine much of the same information from a polycrystalline

sample that would normally require single crystal rotation, one can obtain information not available from the single crystal rotation studies since one relates the chemical shift principal-axis frame directly to the molecular frame in the present experiments.

#### FINAL COMMENTS

A review of the experimental capabilities presently available for the modification of spin Hamiltonians normally encountered in solids has been presented to illustrate the control the still-developing high-resolution, solid state NMR techniques furnish. Examples have been discussed to furnish insight into how such schemes can be used to control the time development of a nuclear spin system to allow a detailed characterization of both the electronic and molecular-frame structure near a nuclear site. While the examples specifically discussed have been chosen from areas of current activity, they are only examples of present efforts, and future developments in this field will undoubtedly furnish many more such examples since the concepts upon which these techniques are based are quite general, and there exists great flexibility for the development of specific experimental schemes for a given problem.

Acknowledgments

Portions of this work were supported by the Office of Naval Research, the National Science Foundation, and the Energy Research and Development Administration. Additional support as an Alfred P. Sloan Foundation Fellow and receipt of a Camille and Henry Dreyfus Foundation Teacher Scholar grant are also acknowledged.

Literature Cited

1. Mehring, M. 1976. NMR--Basic Principles and Progress 11:1-235
2. Haeblerlen, U. 1976. Adv. Mag. Resonance Supplement 1:1-186
3. Griffin, R. G. 1977. Anal. Chem. 49:951A-960A
4. Vaughan, R. W. 1974. Ann. Rev. of Matr. Sci. 4:21-41
5. Andrew, E. R. 1971. Progr. NMR Spectrosc. 8:1-39
6. Mansfield, P. 1971. Progr. NMR Spectrosc. 8:41-101
7. Abragam, A. 1961. The Principles of Nuclear Magnetism. London: Oxford University Press
8. Slichter, C. P. 1963. Principles of Magnetic Resonance. New York: Harper and Row
9. Taylor, P. C., Baugher, J. F., Kriz, H. M. 1975. Chem. Reviews 75:203-240
10. Goldman, M. 1970. Spin Temperature and Nuclear Magnetic Resonance in Solids. London: Oxford University Press
11. Ailion, D. C. 1971. Advan. Magn. Resonance 5:177-227
12. McCall, D. W. 1971. Accounts Chem. Res. 4:223-232
13. Allen, P. S. 1972. IUP International Review of Science--Physical Chemistry Section, ed. C. A. McDowell, 4:43-83. London: Butterworth
14. Pfeifer, H. 1972. NMR: Basic Principles and Progress, ed. P. Diehl, E. Fluck, R. Kosfeld, 7:53-153. New York: Springer-Verlag
15. Resing, H. A. 1967. Advan. Mol. Relaxation Processes 1:109-154
16. Stokes, H. T., Ailion, D. C. 1977. Phys. Rev. Letters 38:1159-1161
17. Stokes, H. T., Ailion, D. C. 1977. Phys. Rev. B 15:1271-1282
18. Stokes, H. T., Ailion, D. C. 1977. Phys. Rev. B 16:3056-3060
19. Muller, R., Willisch, R. 1976. J. Mag. Reson. 21:135-142
20. Broekaert, P., Jeener, J. 1977. Phys. Rev. B 15:4168-4173
21. Woessner, D. E. 1977. Mol. Phys. 34:899-920
22. Wolf, D. 1977. Phys. Rev. B 14:932-944; Wolf, D., Figueroa, D. R., Strange, J. H. 1977. Phys. Rev. B 15:2545-2558
23. Rhim, W.-K., Burum, D. P., Elleman, D. D. 1976. Proceedings of the XIX<sup>th</sup> Congress Appéere Heidelberg, September, 225-228
24. Rhim, W.-K., Burum, D. P., Elleman, D. D. 1976. Phys. Rev. Letters 37:1764-1766
25. Rhim, W.-K., Burum, D. P., Elleman, D. D. 1978. J. Chem. Phys. (in press)
26. Vega, A. J., Vaughan, R. W. 1978. J. Chem. Phys. (in press)

27. Lind, A. C. 1977. J. Chem. Phys. 66:3482-3490
28. Vaughan, R. W., Elleman, D. D., Stacey, L. M., Rhim, W.-K., Lee, J. W. 1972. Rev. Sci. Instrum. 43:1356-1364; Stoll, M. E., Vega, A. J., Vaughan, R. W. 1977. Rev. Sci. Instrum. 48:800-803
29. Ellett, J. D., Jr., et al. 1971. Advances in Magnetic Resonance, ed. J. S. Waugh, 5:117-228. New York; Academic; Cross, V. R., Hester, R. K., Waugh, J. S. 1976. Rev. Sci. Instrum. 47:1486-1489
30. Pines, A., Gibby, M. G., Waugh, J. S. 1973. J. Chem. Phys. 59:569-590
31. Rhim, W.-K., Elleman, D. D., Schreiber, L. B., Vaughan, R. W. 1974. J. Chem. Phys. 60:4595-4604
32. Andrew, E. R., Bradbury, A., Eades, R. G. 1959. Nature 183:1802-1803
33. Lowe, I. J. 1959. Phys. Rev. Letters 2:285-287
34. Granel, P. K., Mansfield, P., Whitaker, M. A. B. 1973. Phys. Rev. B 8:4149-4163
35. Bleich, H. E., Redfield, A. G. 1971. J. Chem. Phys. 55:5405-5406
36. Bleich, H. E., Redfield, A. G. 1977. J. Chem. Phys. 67:5040-5047
37. Hartmann, S. R., Hahn, E. L. 1962. Phys. Rev. 128:2042-2053
38. Boden, N., Levine, Y. K. 1975. Mol. Phys. 29:1221-1227
39. Mehring, M., Sinning, G., Pines, A. 1976. Z. Physik B 24:73-76
40. Sinning, G., Mehring, M., Pines, A. 1976. Chem. Phys. Letters 43:362-386
41. Mehring, M., Sinning, G. 1977. Phys. Rev. B 15:2519-2532
42. Spiess, H. W., Haeblerlen, U., Zimmermann, H. 1977. J. Mag. Reson. 25:55-66
43. Appleman, B. R., Dailey, B. P. 1974. Adv. Magn. Resonance 7:231-320
44. Ditchfield, R. 1976. A Specialist's Periodical Report: Nuclear Magnetic Resonance, ed. R. K. Harris, 5:1-57. London: Burlington House, The Chemical Society
45. Ryan, L. M., Wilson, R. C., Gerstein, B. C. 1977. J. Chem. Phys. 67:4310-4311; Ryan, L. M., Wilson, R. C., Gerstein, B. C. 1977. Chem. Phys. Letters 52:341-344
46. Van Hecke, P., Spiess, H. W., Haeblerlen, U. 1976. J. Mag. Reson. 22:93-102; ibid 22:103-116
47. Raber, H., Mehring, M. 1977. Chem. Phys. Letters 49:498-500; ibid, 1977. Chem. Phys. 26:123-130
48. Dybowski, C. R., Gerstein, B. C., Vaughan, R. W. 1977. J. Chem. Phys. 67:3412-3415
49. Lau, K.-F., Vaughan, R. W., Satterthwaite, C. B. 1977. Phys. Rev. B 15:2449-2457

50. Hfcol, A. T., Vaughan, R. W. 1978. ACS Symposium Series, "Metal Hydrides"  
ed. B. Bau. (in press). American Chemical Society
51. Lau, K-F., Vaughan, R. W. 1976. J. Chem. Phys. 65:4825-4829
52. Torman, J. V. D., Veeman, W. S., DeBoer, E. 1977. Chem. Phys. 24:45-49
53. Wolff, E. K. Griffin, R. G., Kaugh, J. S. 1977. J. Chem. Phys. 67:2387-2388
54. Halstead, T. K., Spiess, H.W., Haeblerlen, U. 1976. Mol. Phys. 31:1569-1583
55. VanderHart, D. L. 1976. J. Chem. Phys. 64:830-834
56. Yannoni, C. S., Vieth, H-M. 1976. Proceedings of the XIXth Congress  
Ampère Heidelberg, September 1976, 437-440
57. Pines, A., Ruber, D. J., Vega, S., Mehring, M. 1976. Phys. Rev. Letters  
36:110-113
58. Pines, A., Vega, S., Ruben, D. J., Shattuck, T. W., Wenner, D. W. 1976.  
Magnetic Resonance in Condensed Matter---Recent Developments (Proceedings of  
the 17th Ampère International Summer School, Pula, Yugoslavia, September,  
1976), 127-179
59. Vega, S., Shattuck, T. W., Pines, A. 1976. Phys. Rev. Letters 37:43-46
60. Vega, S., Pines, A. 1977. J. Chem. Phys. 66:5624-5644; ibid. 1976.  
Proceedings of the XIXth Congress Ampère, Heidelberg, September 1976,  
395-400
61. Kunitomo, M. 1971. J. Phys. Soc. Japan 30:1059-1067
62. Burum, D. P., Elleman, D. D., Rhim, W-K. 1978. J. Chem. Phys. (in press)
63. Terao, T., Hashi, T. 1974. J. Phys. Soc. Japan 36:989-999; ibid. 1972.  
J. Mag. Reson. 7:238-240
64. Sears, R. E. J. 1974. J. Chem. Phys. 61:4368-4369; ibid. 1973. J. Chem.  
Phys. 59: 5213-5214; ibid. 1973. J. Chem. Phys. 59:973-974
65. Humpheries, L. J., Sears, R. E. J. 1975. J. Phys. Chem. Solids 36:1149
66. Becker, J., Sowelack, Mehring, M. 1978. (in press)
67. Blinc, R., Burgar, M., Rutar, V. Selinger, J., Zupancic, I. 1977.  
Phys. Rev. Letters 38:92-95
68. Schaefer, J., Stejskal, E. O., Buchdahl, R. 1975. Macromolecules 8:291-296
69. Schaefer, J., Stejskal, E. O., Buchdahl, R. 1977. Macromolecules 10: 384-405
70. Schaefer, J., Stejskal, E. O., Buchdahl, R. 1977. J. Macromol. Sci. Phys.  
(in press)
71. Garroway, A. N., Moniz, W. B., Resing, H. A. 1976. Organic Coatings and  
Plastics. Preprints, 172th National American Chemical Society Meeting,  
San Francisco, September 1976, 133-139
72. VanderHart, D. L. 1976. J. Mag. Reson. 24:467-470

73. Torchia, D. A., Vanderhart, D. L. 1976. J. Molec. Biology 104:315-321; ibid. 1976. Topics in Carbon-13 NMR Spectroscopy, ed. G. C. Levy (in press)
74. Bartuska, V. J., Maciel, G. E., Schaefer, J. Stejskal, E. O. 1977. Fuel 56:354-358
75. VanderHart, D. L., Retcofsky, H. L. 1976. Fuel 55:202-204; ibid. 1976. Proceedings of the Coal Chemistry Workshop at Stanford Research Institute, 202
76. Retcofsky, H. L., Vanderhart, D. L. 1978. Fuel (in press)
77. Resing, H. A., Garroway, A. J., Hazlett, R. N. 1978. Fuel (in press)
78. Schreiber, L. B., Vaughan, R. W. 1975. J. Catal. 40:226-235; Vaughan, R. W., Schreiber, L. B., Schwarz, J. A. 1976. ACS Symposium Series: Magnetic Resonance in Colloid and Interface Science, ed. H. A. Resing and C. G. Wade 34:275-289. American Chemical Society
79. Sefcik, M. D., Schaefer, J., Stejskal, E. O. 1977. ACS Symposium Series: Molecular Sieves--II, ed. J. R. Katzer 40:344-356. American Chemical Society
80. Whipple, E. B., Green, P. J., Ruta, M., Bujalski, R. L. 1976. J. Phys. Chem. 80:1350-1356
81. Griffin, R. G. 1976. J. Am. Chem. Soc. 98:851-852; Herzfeld, J., Griffin, R. G., Haberkorn, R. A. 1978. Biochemistry (in press); Griffin, R. G., Powers, L., Pershan, P. S. 1978. Biochemistry (in press)
82. Kohler, S. J., Klein, M. P. 1976. Biochemistry 15:967-973; ibid. 1977. Biochemistry 16:519-526
83. Seelig, J., Galley, H. U. 1976. Eiochemistry 15:5199-5204
84. Cohen, M. H., Reif, F. 1957. Solid State Physics, ed. F. Seitz and D. Turnbull 5:321-438. New York: Academic
85. Goldstein, H. 1950. Classical Physics, 107-109. Reading, Mass.: Addison-Wesley
86. Mehring, M., Raber, H. 1973. Proceedings of the First Specialized Colloque Ampère, Krakow, August 1973, ed. J. W. Henne1, 216-219
87. Hatanaka, H., Terao, T., Hashi, T. 1975. J. Phys. Soc. Japan 39:835-836
88. Hatanaka, H., Hashi, T. 1975. J. Phys. Soc. Japan 39: 1139-1140
89. Hatanaka, H., Ozawa, T., Hashi, T. 1977. J. Phys. Soc. Japan 43: 2069-2070
90. Blinc, R., Rutar, V., Seliger, J. Siak, J. Smolej, V. 1977. Chem. Phys. Letters 48:576-578

91. Berglund, B., Tegenfeldt, J. 1977. J. Magn. Reson. 27:315-323
92. Wolff, E. K., Griffin, R. G., Watson, C. 1977. J. Chem. Phys. 66:5433-5438
93. Van Willigen, H., Haberkorn, R. A., Griffin, R. G. 1977. J. Chem. Phys. 67:917-924; Stark, R. E., Haberkorn, R. A., Griffin, R. G. 1978 (in press)
94. Polak, M., Vaughan, R. W. 1977. Phys. Rev. Letters 39:1677-1680
95. Stoll, M. E., Vega, A. J., Vaughan, R. W. 1977. Phys. Rev. A 16:1521-1524
96. Schaefer, J., Stejskal, E. O. 1976. J. Am. Chem. Soc. 98:1031-1032
97. Lipmaa, E., Ailla, M., Tuherm, T. 1976. Proceedings of the XIXth Congress Ampere, Heidelberg, September 1976, 113-118
98. Stejskal, E. O., Schaefer, J., McKay, R. A. 1977. J. Mag. Reson. 25:569-573
99. Ailla, M., Lipmaa, E. 1976. Chem. Phys. Letters 37:260-264
100. Mariq, M., Waugh, J. S. 1977. Chem. Phys. Letters 47:327-329
101. Figure 4 is from unpublished results of R. A. Haberkorn, J. Herzfeld, and R. G. Griffin
102. Schnabel, B., Haubenreisser, U., Scheier, G., Müller, R. 1976. Proceedings of the XIXth Congress Ampere, Heidelberg, 1976, 441-444
103. Gerstein, B. C., Pembleton, R. G., Wilson, R. C., Ryan, L. M. 1977. J. Chem. Phys. 66:361-362
104. Haberkorn, R. A., Herzfeld, J., Griffin, R. G. 1978. (in press)
105. Garrowsay, A. N. 1978. J. Magn. Reson. (in press)
106. Stejskal, E. O., Schaefer, J. 1977. J. Magn. Reson. 28:105-112
107. Stoll, M. E., Vega, A. J., Vaughan, R. W. 1976. J. Chem. Phys. 65:4033-4098
108. Stoll, M. E., Vega, A. J., Vaughan, R. W. 1976. Proceedings of the XIXth Congress Ampere, Heidelberg, 1976, 429-432
109. Aue, W. P., Bartholdi, E., Ernst, R. R. 1976. J. Chem. Phys. 64:2229-2246
110. Hokaun, A., Ernst, R. R. 1977. J. Chem. Phys. 67:1752-1758
111. Backmann, P., Aue, W. P., Müller, L., Ernst, R. R. 1977. J. Magn. Reson. 28:29-39
112. Hester, R. K., Ackerman, J. L., Neff, B. L., Waugh, J. S. 1976. Phys. Rev. Letters 36:1081-1083
113. Opeila, S. J., Waugh, J. S. 1977. J. Chem. Phys. 66:4919-4924
114. Rybaczewski, E. F., Neff, B. L., Waugh, J. S. Sherfinski, J. S. 1977. J. Chem. Phys. 67:1231-1236
115. Van Willigen, H., Griffin, R. G., Haberkorn, R. A. 1978. (in press)
116. Müller, L., Kumar, A., Baumann, T., Ernst, R. R. 1974. Phys. Rev. Letters 32:1402-1406
117. Hester, R. K., Ackerman, J. L., Cross, V. R., Waugh, J. S. Phys. Rev. Letters 34:993-996
118. Lee, M. Goldberg, W. I. 1965. Phys. Rev. 140:A1261-A1271
119. Stoll, M. E., Rhim, W.-K., Vaughan, R. W. 1976. J. Chem. Phys. 64:4808-4809

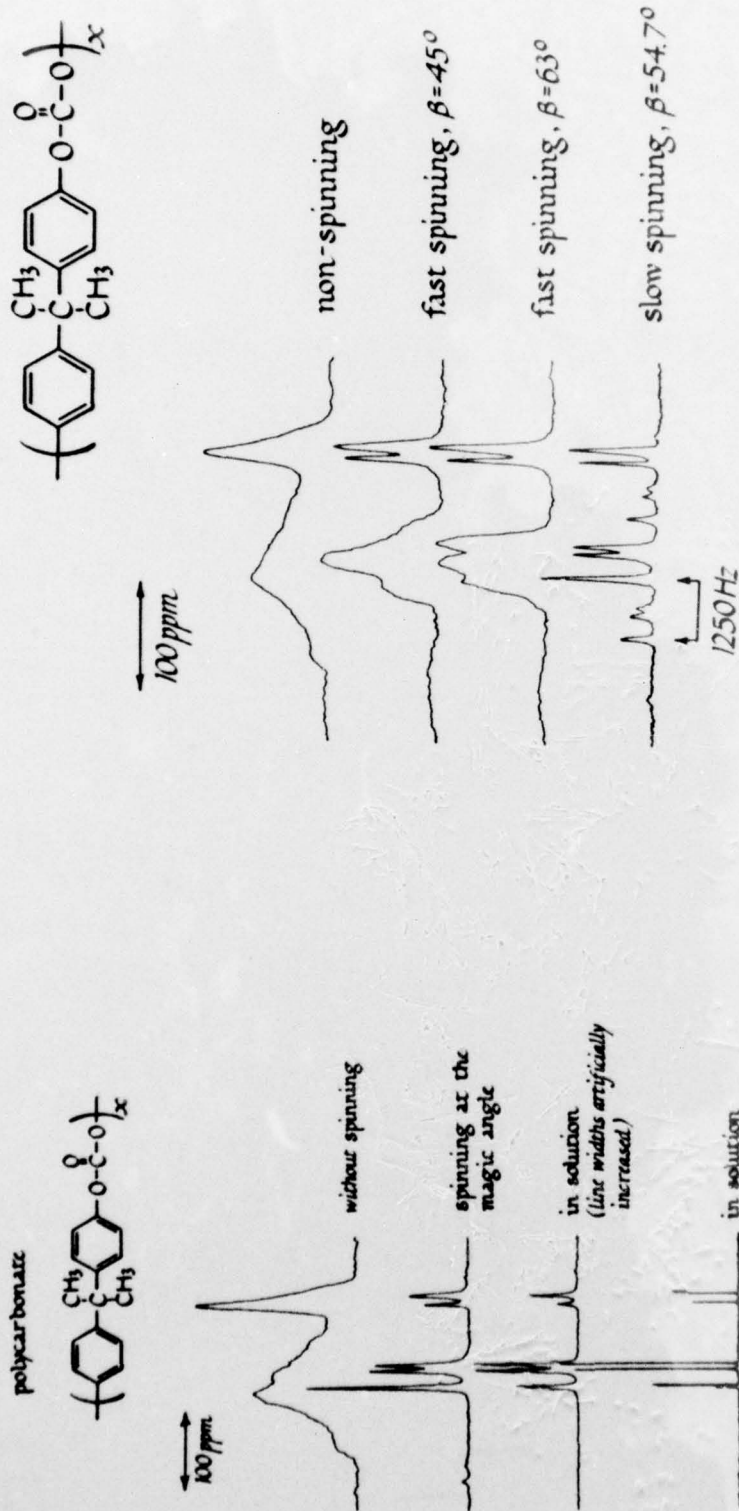


Figure 1. Cross-polarization  $^{13}\text{C}$  spectra of polycarbonate, with and without magic-angle spinning. The CP spectra are compared to a spectrum of the polymer in solution (with solvent lines omitted for clarity of presentation). The liquid spectrum is not fully relaxed. (From reference 69)

Figure 2. Dipolar-decoupled, cross-polarization  $^{13}\text{C}$  NMR spectra of a polycarbonate rotor under a variety of spinning conditions. The fast spinning frequency was 3.2 kHz, and the slow spinning frequency was 1250 Hz. (From reference 98)

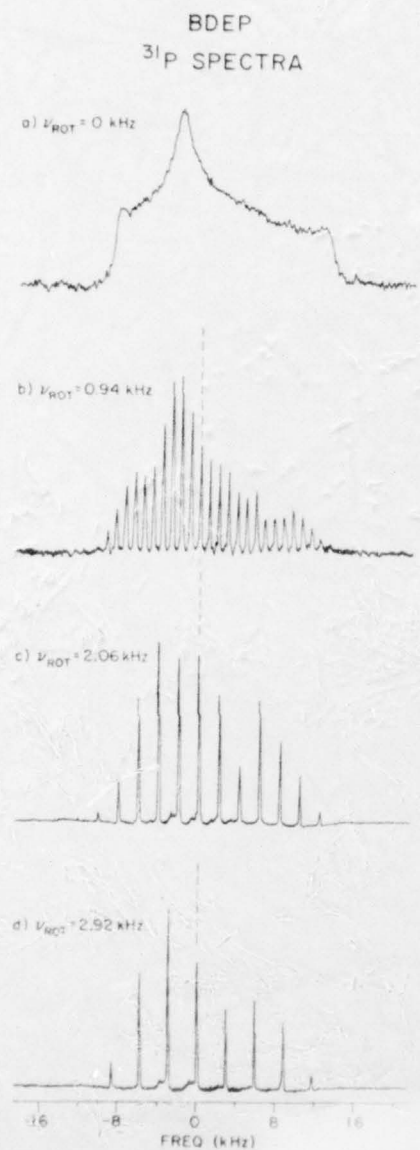


Figure 3. <sup>31</sup>P chemical shift spectra of barium diethylphosphate (BDEP) taken at 119.05 MHz, as a function of sample rotation frequency. (From unpublished results of R. A. Haberkorn, J. Herzfeld, and R. G. Griffin)

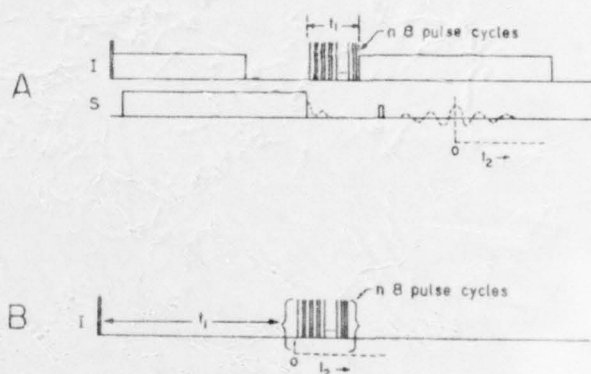


Figure 4. The pulsing sequences used in: (A) the heteronuclear dipolar vs. dilute spin chemical shift, and (B) the homonuclear dipolar vs. abundant-spin chemical shift experiments.

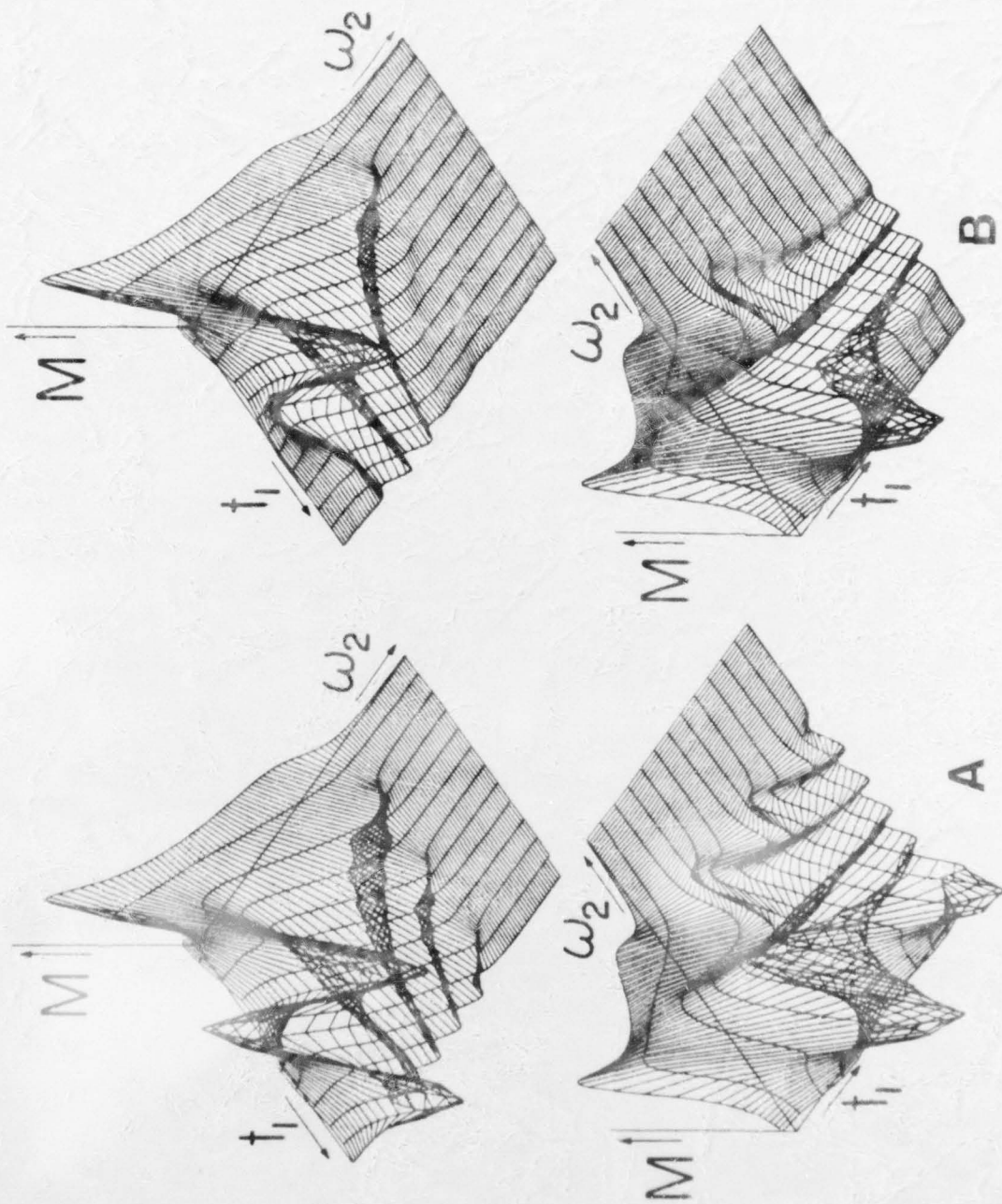


Figure 5. Theoretical heteronuclear dipolar-modulated chemical shift spectra for the  $^{13}\text{C}$  resonance in benzene. Calculation (A) considered only a single  $^{13}\text{C}$ - $^1\text{H}$  dipolar interaction, while calculation (B) included the other  $^{13}\text{C}$ - $^1\text{H}$  dipolar terms within the benzene molecule. (Unpublished figure of M. E. Stoll, A. J. Vega, and R. W. Vaughan)

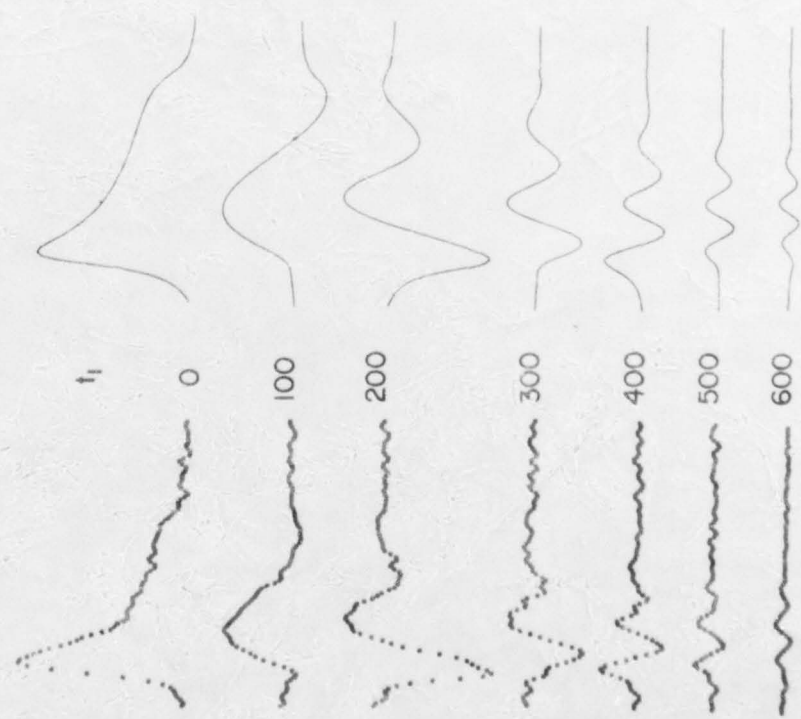


Figure 6. Comparison of calculated and experimental  $^{13}\text{C}$  spectra from benzene as a function of the dipolar evolution time,  $t_1$ . (From reference 108)

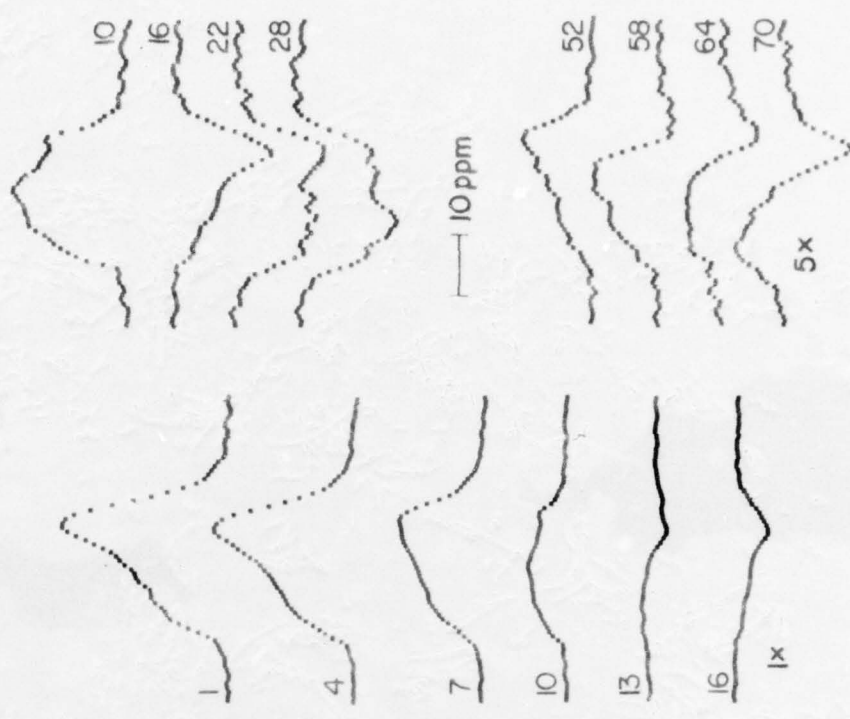


Figure 7. Experimental homonuclear dipolar-modulated chemical shift spectra for  $^1\text{H}$  in  $\text{CCl}_3\text{COOH}$ . The number near each spectrum designates, when multiplied by 4.17 microseconds, the dipolar evolution time,  $t_1$ . (From reference 108)

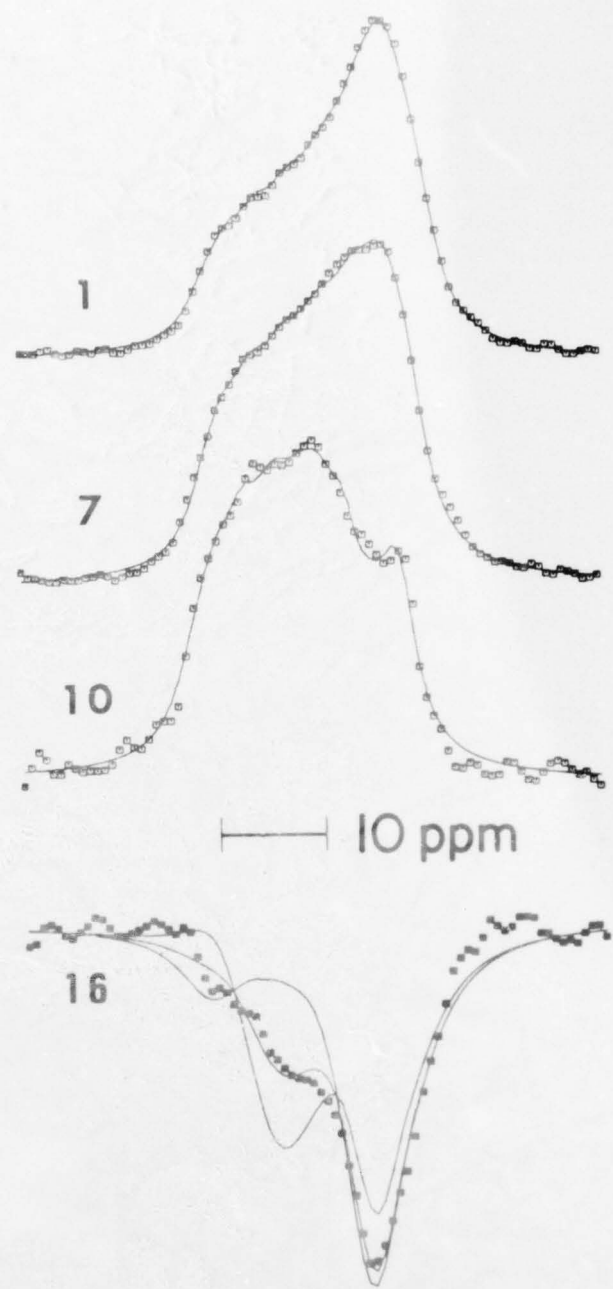


Figure 8. Theoretical fits to four of the homonuclear dipolar-modulated proton chemical shift spectra from Figure 7. The number near each spectrum designates, when multiplied by 4.17 microseconds, the dipolar evolution time,  $t_1$ . The three curves through the data in the power spectrum are to illustrate the sensitivity of the fits to the orientation of the proton-proton vector in the chemical shift principal axis frame. To obtain the two lines which do not fit the spectrum, the value of the angle between the axis of unique component of the chemical shift tensor and the proton-proton vector has been altered by  $\pm 3^\circ$  from the correct value (which gives the best fit to the data). (Unpublished results of M. E. Stoll, A. J. Vega, and R. W. Vaughan)

TECHNICAL REPORT DISTRIBUTION LIST

No. Copies

Office of Naval Research Arlington, Virginia 22217 Attn: Code 472	2	Defense Documentation Center Building 5, Cameron Station Alexandria, Virginia 22304
Office of Naval Research Arlington, Virginia 22217 Attn: Code 102IP 1	6	U.S. Army Research Office P.O. Box 12211 Research Triangle Park, NC 27709 Attn: CRD-AA-IP
ONR Branch Office 536 S. Clark Street Chicago, Illinois 60605 Attn: Dr. Jerry Smith	1	Naval Ocean Systems Center San Diego, California 92161 Attn: Mr. Joe McCartney
ONR Branch Office 715 Broadway New York, New York 10003 Attn: Scientific Dept.	1	Naval Weapons Center China Lake, California 93550 Attn: Head, Chemistry Division
ONR Branch Office 1030 East Green Street Pasadena, California 91106 Attn: Dr. R. J. Marcus	1	Naval Civil Engineering Laboratory Port Hueneme, California 94923 Attn: Mr. W. S. Haynes
ONR Branch Office 760 Market Street, Rm. 447 San Francisco, California 94102 Attn: Dr. P. A. Miller	1	Professor O. Heinz Department of Physics & Chemistry Naval Postgraduate School Monterey, California 93943
ONR Branch Office 495 Summer Street Boston, Massachusetts 02210 Attn: Dr. L. H. Peebles	1	Dr. A. L. Slafkosky Scientific Advisor Commandant of the Marine Corps Washington, D.C. 20380
Director, Naval Research Laboratory Washington, D.C. 20390 Attn: Code 6100	1	Office of Naval Research Arlington, Virginia 22217 Attn: Dr. Richard S. Mill
The Asst. Secretary of the Navy (R&D) Department of the Navy Room 4E736, Pentagon Washington, D.C. 20350	1	
Commander, Naval Air Systems Command Department of the Navy Washington, D.C. 20360 Attn: Code 310C (H. Rosenwasser)	1	

TECHNICAL REPORT DISTRIBUTION LIST

No. Copies

No. Copies

TECHNICAL REPORT DISTRIBUTION LIST

No. Copies

No. Copies

Dr. D. A. Vroom IAT P.O. Box 80817 San Diego, California 92138	1	Dr. R. W. Vaughan California Institute of Technology Division of Chemistry & Chemical Engineering Pasadena, California 91125	1	Dr. Leonard Kharton James Franck Institute Department of Chemistry 5640 Ellis Avenue Chicago, Illinois 60637	1
Dr. G. A. Somorjai University of California Department of Chemistry Berkeley, California 94720	1	Dr. Keith H. Johnson Massachusetts Institute of Technology Department of Metallurgy and Materials Science Cambridge, Massachusetts 02139	1	Dr. M. G. Legally Department of Metallurgical and Mining Engineering University of Wisconsin Madison, Wisconsin 53706	1
Dr. L. M. Jarvis Surface Chemistry Division 4555 Overlook Avenue, S.W. Washington, D.C. 20375	1	Dr. M. S. Wrighton Massachusetts Institute of Technology Department of Chemistry Cambridge, Massachusetts 02139	1	Dr. Robert Goner James Franck Institute Department of Chemistry 5640 Ellis Avenue Chicago, Illinois 60637	1
Dr. W. M. Risen, Jr. Brown University Department of Chemistry Providence, Rhode Island 02912	1	Dr. J. E. Demuth IBM Corp. Thomas J. Watson Research Center P.O. Box 218 Yorktown Heights, New York 10598	1	Dr. R. F. Wallis University of California (Irvine) Department of Physics Irvine, California 92664	1
Dr. M. K. Chisholm Princeton University Chemistry Department Princeton, New Jersey 08540	1	Dr. C. P. Flynn University of Illinois Department of Physics Urbana, Illinois 61801	1		
Dr. J. B. Hudson Rensselaer Polytechnic Institute Materials Division Troy, New York 12181	1	Dr. W. Kohn University of California (San Diego) Department of Physics La Jolla, California 92037	1		
Dr. John T. Yates National Bureau of Standards Department of Commerce Surface Chemistry Section Washington, D.C. 20234	1	Dr. R. L. Park Director, Center of Materials Research University of Maryland College Park, Maryland 20742	1		
Dr. Theodore E. Medey Department of Commerce National Bureau of Standards Surface Chemistry Section Washington, D.C. 20234	1				
Dr. J. M. White University of Texas Department of Chemistry Austin, Texas 78712	1				
		Dr. W. T. Perla Electrical Engineering Department University of Minnesota Minneapolis, Minnesota 55455	1		
		Dr. Markis Tzoar City University of New York Convent Avenue at 138th Street New York, New York 10031	1		
		Dr. Chia-wei Woo Northwestern University Department of Physics Evanston, Illinois 60201	1		
		Dr. D. C. Mattis Yeshiva University Physics Department Amsterdam Avenue & 185th Street New York, New York 10033	1		
		Dr. Robert M. Hexter University of Minnesota Department of Chemistry Minneapolis, Minnesota 55455	1		

San Francisco, California 941  
Attn: Dr. P. A. Miller

ONR Branch Office  
495 Summer Street  
Boston, Massachusetts 02210  
Attn: Dr. L. H. Peebles

Director, Naval Research Labor  
Washington, D.C. 20390  
Attn: Code 6100

The Asst. Secretary of the Nav,  
Department of the Navy  
Room 4E736, Pentagon  
Washington, D.C. 20350

Commander, Naval Air Systems Co  
Department of the Navy  
Washington, D.C. 20360  
Attn: Code 310C (H. Rosenwasse

